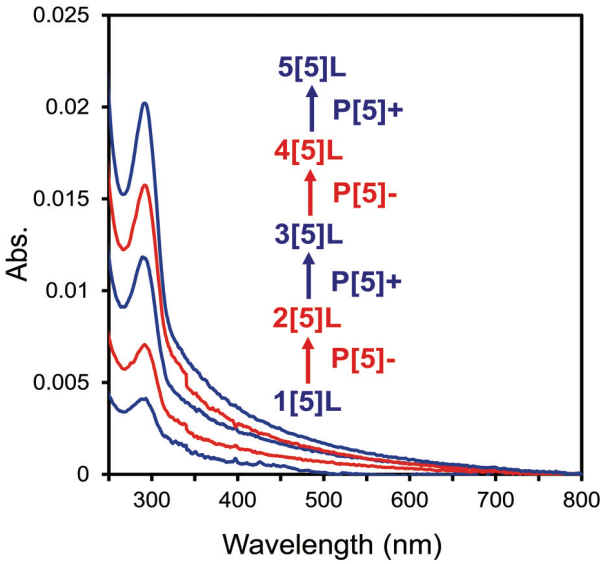

Supplementary Figure 1 UV-vis absorption spectra of the film by consecutive adsorption of **P[5]+** and **P[5]-**.

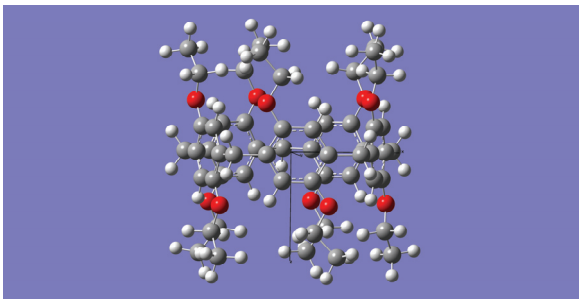

State	X	Y	Z	Oscillator Strength	Wavelength (nm)
1	-0.0053	0.0004	0.4892	0.0242	301.01
2	-1.2166	0.1856	0.0013	0.1593	288.88
3	-0.1859	-1.2175	-0.0005	0.1595	288.83
4	-0.0109	0.0020	0.0019	0.0000	279.02
5	-0.0029	-0.0123	-0.0006	0.0000	279.00
6	0.6843	0.1075	-0.0064	0.0532	274.21
7	0.1094	-0.6837	-0.0019	0.0531	274.08
8	0.0009	0.0189	0.0001	0.0000	271.02
9	-0.0119	0.0020	-0.2100	0.0050	269.37
10	-0.0035	-0.0090	-0.0042	0.0000	268.42
11	-0.0099	0.0037	0.0263	0.0001	268.36
12	-0.0184	0.0038	0.0069	0.0000	261.93
13	0.0002	0.0106	0.0013	0.0000	261.89
14	-0.0609	0.5432	0.0009	0.0348	261.17
15	0.5338	0.0610	-0.0033	0.0336	261.06
16	-0.0090	0.0002	-0.0022	0.0000	256.16
17	-0.0003	-0.0014	-0.0004	0.0000	256.14
18	0.0327	-0.1146	0.0001	0.0017	253.48
19	-0.1170	-0.0320	-0.0009	0.0018	253.45
20	0.0010	-0.0001	0.2087	0.0053	248.77

Supplementary Figure 2 Optimized ground-state structure [M06-2X/6-31G(d,p)] and calculated ground to excited state transition electronic dipole moments [M06/6-311G(d,p)//M06-2X/6-31G(d,p)] of pillar[5]arene with 10 ethoxy groups.

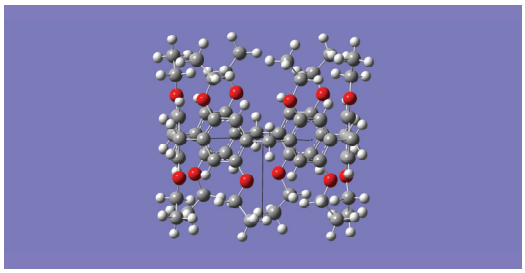

State	X	Y	Z	Oscillator Strength	Wavelength (nm)
1	0.0000	0.0000	-0.5224	0.0282	293.96
2	-0.0634	1.5906	0.0000	0.2697	285.43
3	1.5949	0.0632	0.0000	0.2711	285.40
4	0.0001	0.0000	0.0028	0.0000	277.15
5	0.0000	0.0000	-0.0001	0.0000	277.14
6	0.0004	0.0002	0.0000	0.0000	273.39
7	0.0145	-0.4686	0.0000	0.0245	273.05
8	0.4724	0.0143	0.0000	0.0249	273.04
9	-0.0001	0.0000	0.0000	0.0000	272.16
10	0.0000	0.0000	0.1879	0.0040	269.15
11	0.0000	0.0000	0.0029	0.0000	269.02
12	0.0000	-0.0001	-0.0273	0.0001	269.02
13	-0.0031	0.0004	0.0000	0.0000	266.21
14	0.1091	0.6927	0.0000	0.0568	263.05
15	0.6950	-0.1085	0.0000	0.0571	263.04
16	0.0002	-0.0109	0.0000	0.0000	262.14
17	0.0000	0.0000	0.0035	0.0000	261.31
18	0.0000	0.0000	-0.0001	0.0000	261.26
19	0.0000	0.0002	0.0013	0.0000	257.22
20	0.0001	0.0000	0.0000	0.0000	257.20

Supplementary Figure 3 Optimized ground-state structure [M06-2X/6-31G(d,p)] and calculated ground to excited state transition electronic dipole moments [M06/6-311G(d,p)//M06-2X/6-31G(d,p)] of pillar[6]arene with 12 ethoxy groups.

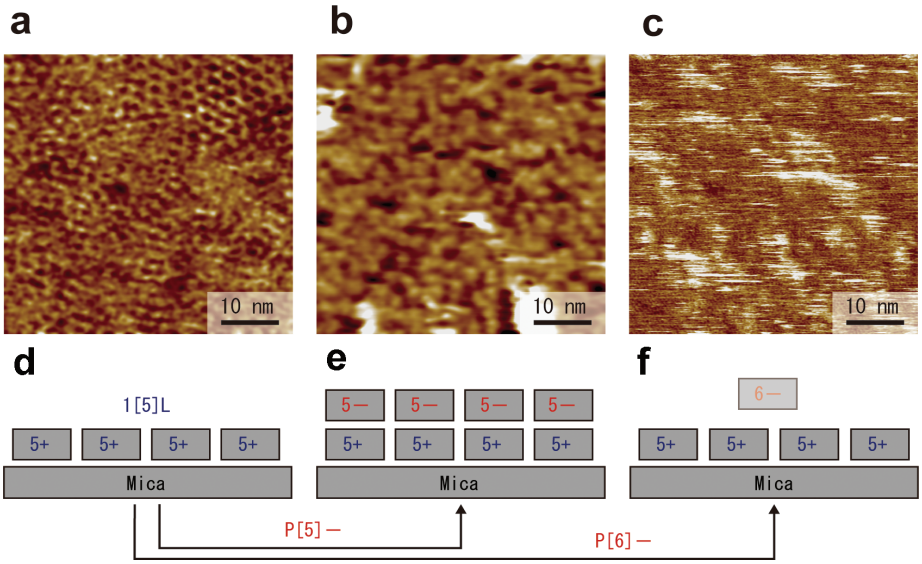

Supplementary Figure 4 FM-AFM images of **a**, the monolayer film **1[5]L**, the films after immersing in an aqueous solution containing **b**, P[**5]-** or **c, P[6]-**. The illustration of **d,** monolayer formation using **P[5]+**, **e,** bilayer formation by immersing in an aqueous solution containing **P[5]-**, **f,** no formation of bilayer after immersing in an aqueous solution containing **P[6]-**.

Supplementary Note 1 Clear change of surface structures was observed after immersion of **1[5]L** film to a solution containing **P[5]-**, suggesting formation of the bilayer film. However, the resolution of the AFM image was low compared with **1[5]L** film because **P[5]-** molecules on **1[5]L** film were not directly adsorbed on the substrate and thus would have larger fluctuation and higher mobility than **P[5]+** molecules on the substrate. In addition, the surface structures of the bilayer film were larger than the monolayer film. Thus, we speculate that the low resolution of the bilayer film was caused by tip contamination during the tip scanning due to the higher structures and higher mobility of **P[5]-** molecules than **P[5]+** molecules on the substrate.

In contrast, the clear surface structure was not observed after immersion of **1[5]L** film to a solution containing **P[6]-**. The AFM image showed the existence of adsorbed structures with high mobility at the surface. These results suggested that the bilayer film did not form, and small amounts of **P[6]A-** molecules may be adsorbed on the surface of **1[5]L** film by the weak electrostatic interaction.

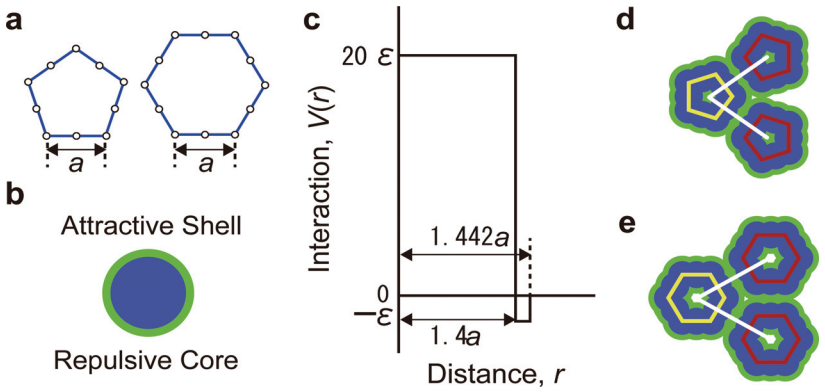

Supplementary Figure 5 Model molecules **1[5]L** or **1[6]L**. **a,** Model molecules **1[5]L** and **1[6]L** represented by regular pentagons and hexagons, respectively, with an edge-length equal to a. **b,** A particle as interaction centres with a repulsive core and an attractive shell, which is placed at the vertices of the polygons or at the middle points of neighbouring vertices. **c,** An isotropic pair-potential $V(r)$ between the particles. **d, e,** Schematic of model molecules **1[5]L** and **1[6]L**, respectively, with the repulsive blue and attractive green regions. Edges of polygons tend to be parallel each other. Because of the polygonal shape a void is produce in the case of **1[5]L**. White lines connecting molecules are guides to the eye.

Supplementary Note 2 Model molecules mimicking **1[5]L** or **1[6]L** are represented by regular pentagons or hexagons, respectively, with an edge-length equal to *a* as shown in Supplementary Figure 5a. For π– π interactions between molecules, we assume a toy model for the interactions: Spherical particles as interaction centres illustrated in Supplementary Figure 5b are placed at the vertices of the polygons and also at the middle points of neighbouring vertices (Supplementary Figure 5b). An isotropic pair-potential V(r) between the particles consists of an inner repulsive-core (blue) and an outer thin attractive-shell (green) shown in Supplementary Figure 5c is the following equation (1):

$$V(r) = \begin{cases} 20\varepsilon & r \le 1.4a \\ -\varepsilon & 1.4a \le r \le 1.442a \end{cases} \qquad (1)$$

The number of particles for a pentagon and a hexagon is ten and twelve, respectively, shown in Supplementary Figure 5a. Accordingly, schematic drawings of the model molecules with the above potentials are illustrated in Supplementary Figures 5d and e, respectively, where the potential between particles acts as the π– π interactions, thereby forcing the edges of red polygons in Supplementary Figures 5d and e parallel at certain

distances. At low temperatures, the attractive-shells tend to touch each other, however, the repulsive-cores hardly contact with the core of other molecules.